Geophys. J. R. astr. Soc. (1978) **52**, 479–501

Transient and impulse responses of a one-dimensional linearly attenuating medium – I. Analytical results

J. B. Minster *Seismological Laboratory, Division of Geological and Planetary Sciences, California Institute of Technology, Pasadena, California 91125, USA*

Received 1977 August 19; in original form 1977 May 18

Summary. The transient and impulse responses (Green's function) for one-dimensional wave propagation in a standard linear solid are calculated using a Laplace Transform method. The spectrum of relaxation times is chosen so as to model a constant Q medium within an absorption band covering a broad frequency range which may be chosen so as to include the seismic frequencies. The inverse transform may be evaluated asymptotically in the limit of very long propagation times using the saddle point method. For shorter propagation times the method of steepest descent may be modified so as to yield an accurate first motion approximation. The character of the small amplitude precursor to the large amplitude 'visible' signal is investigated analytically. It is shown that the signal velocity is intermediate between the high-frequency ('unrelaxed') and the low-frequency ('relaxed') limits of the phase velocity.

Introduction

The problem of wave propagation in attenuating and dispersive media is well understood, and numerous and detailed studies can be found in the literature, starting with Sommerfeld (1914). Brillouin (1960) gives a detailed account for the case of electromagnetic waves, and a comprehensive review outlining the parallelism between electromagnetic and acoustic problems is presented by Elices & García-Moliner (1968).

Most of the analysis is performed for the propagation of quasi monochromatic waves or for wave packets of a few cycles. The propagation of monochromatic plane waves in linear viscoelastic solids and their interaction with planar interfaces is studied by Schoenberg (1971) and by Borcherdt (1973a, b, 1977) who also considers the question of energy propagation. Buchen (1971) obtained asymptotic solutions for cylindrical waves reflected and refracted at the interface between two linear viscoelastic half-spaces.

On the other hand, for seismic purposes, one often needs the transient (step function) or impulse (delta function) responses of the medium. A large variety of solutions, often constructed on an *ad hoc* basis, are offered in the seismological and mechanical literature, and

yield wave forms with grossly similar characteristics (e.g. Kolsky 1956; Lomnitz 1957; Futterman 1962; Lamb 1962; Savage 1965; Carpenter 1967; Azimi, Kalinin & Pivovarov 1968; Strick 1970). Reviews of such work are provided by Kogan (1966a, b) and more recently by Stacey *et al.* (1975). The latter authors make an attempt at defining criteria which the attenuation operator must satisfy in order to be acceptable in seismology.

In general, the approach is to construct a simple phenomenological law which would yield an adequate representation of relatively complex physical mechanisms and yield a weak dependence of the quality factor Q on frequency over the seismic range (e.g. Anderson 1967; Jackson & Anderson 1970; Anderson & Hart 1977). On the other hand, Liu, Anderson & Kanamori (1976) and Anderson *et al.* (1977) showed how the rheology of a standard linear solid satisfies the observational seismological constraints. These results are confirmed by the extensive modelling work of Anderson & Hart (1977). The constitutive equation of a standard linear solid is the most general linear relation between stress, strain, and their first-time derivatives, and is extensively used in linear viscoelasticity (e.g. Malvern 1969). As discussed in the papers quoted above, such a rheology is consistent with a wide variety of laboratory results and physical models of imperfect elasticity (e.g. partial melting, stress induced reordering, phase changes, intergranular thermoelasticity ...). Anderson & Hart (1977) favour a grain boundary relaxation model which explains most of what is known about attenuation in the Earth's mantle.

Various versions of viscoelastic rheologies have previously been considered (e.g. Chu 1962; Gurevich 1964; Blake 1974 and Blake & Dienes 1976), for plane wave and spherical wave propagation problems. Borcherdt (1973a, b) also makes use of such a model. However, as pointed out by Liu *et al.* (1976) there remains some confusion in the literature as to the detailed character of attenuated plane impulsive waves – the Green's function. Several causes may be invoked for this on the basis of their work: (1) different authors (e.g. Futterman 1962; Strick 1970) have adopted different conventions in order to define the 'non-dispersive' limiting behaviour of the medium, i.e. either the long-period or the high-frequency behaviour; (2) the possible presence of a low amplitude precursor remains somewhat obscure, since the analysis of Strick (1970) pertains to rather *ad hoc* models. In addition, one should point out that many of the proposed solutions require a Fourier transform (FFT) technique or another method of numerical integration, so that the frequency band one can investigate is limited, and is often narrower than the absorption band itself (Liu 1976, private communication). Furthermore, with such methods, small amplitude precursors will be hidden in numerical noise or will not be obtained at all since they originate precisely from frequency components lying outside the absorption band (Elices & García-Moliner 1968).

In this paper we shall investigate in detail the character of attenuated plane impulsive waves. In particular, we shall obtain analytical asymptotic expressions both for the principal wave and for the precursor. The analytical approach avoids all the shortcomings of a numerical approach and allows for an accurate assessment of the effects of various parameters. We shall see that the gross features of the attenuated wave are in general agreement with previously obtained results, but that the actual visual onset time depends critically upon the high frequency side of the absorption band.

Strictly speaking, the approximation used in this paper is only accurate for propagation times longer than the longest period for which dissipation is significant. In practice, we shall see that this restriction affects only the coda of the attenuated pulse, and that the onset is accurately obtained whenever the propagation time is long compared to the shortest period at which significant dissipation occurs. This paper will focus on the analytical investigation and a parameter study involving numerical examples will be published separately in a second part.

1 Formulation of the problem

(a) A standard linear medium may be defined by the following constitutive equation (e.g. Malvern 1969; Liu *et al.* 1976)

$$\frac{\sigma}{\tau_\sigma} + \dot{\sigma} = M_u\left(\frac{\epsilon}{\tau_\epsilon} + \dot{\epsilon}\right), \tag{1.1}$$

where σ is stress, ϵ strain, and M_u a modulus of deformation. M_u controls the 'glassy' behaviour of the material, that is, its instantaneous response to a suddenly applied force or deformation. We call it, as is customary, the 'unrelaxed' modulus. (1.1) is of the most general form of a linear relation between stress, strain, and their first-time derivatives. Since we are primarily interested in the quasi elastic behaviour of the medium, we take the position that M_u is a given quantity, which is characteristic of the material. τ_σ is the stress relaxation time under constant strain, and τ_ϵ is the strain retardation time under constant stress. These quantities control the anelastic properties of the medium; it is easy to verify that the requirement that the material be attenuating implies $\tau_\sigma < \tau_\epsilon$. We shall assume that

$$\frac{\tau_\sigma}{\tau_\epsilon} = 1 - c. \tag{1.2}$$

Let $\mathscr{R}(t)$ be the stress response of the medium to a unit step function strain; we have

$$\mathscr{R}(t) = M_u[\![1 - c\,[1 - \exp(-t/\tau_\sigma)]\,]\!]H(t). \tag{1.3}$$

Thus we see that for $c \ll 1$, the material is solid-like, and the stress reaches a final equilibrium value. For $c \sim 1$ the material is fluid-like, and the stress becomes small in the long-time limit. We are primarily interested in solid-like media.

For the simple case of a linear rheology, (e.g. Rivlin 1965), the Boltzmann after-effect equation may be written

$$\sigma(t) = \int_{-\infty}^{t} \mathscr{R}(t-\tau)\,d\epsilon(\tau), \tag{1.4}$$

where the right-hand side is a Stieltjes integral. For a medium initially at rest and in equilibrium at $t = 0$, this equation may be recast in the form

$$\sigma(t) = \frac{d}{dt}\int_0^{t^+} \mathscr{R}(t-\tau)\,\epsilon(\tau)\,d\tau. \tag{1.5}$$

We introduce the Laplace transform of a function $f(t)$ by

$$f^*(s) = s\int_0^\infty \exp(-st)\,f(t)\,dt. \tag{1.6}$$

In the transformed domain, the Boltzman after-effect equation takes the form

$$\sigma^*(s) = \mathscr{R}^*(s)\,\epsilon^*(s). \tag{1.7}$$

$\mathscr{R}^*(s)$ will be called the operational modulus. For one single relaxation mechanism we have

$$\mathscr{R}^*(s) = M_u\frac{s + \tau_\epsilon^{-1}}{s + \tau_\sigma^{-1}}. \tag{1.8}$$

However, following Gurevich (1964) and Liu *et al.* (1976), we shall assume that there exists a complete spectrum of relaxation mechanisms, operating independently, with the distribution function

$$D(\tau_\sigma) = \begin{cases} D/\tau_\sigma & \text{for} \quad \tau_m < \tau_\sigma < \tau_M, \\ 0 \text{ otherwise.} \end{cases} \tag{1.9}$$

In other words, τ_m^{-1} and τ_M^{-1} are the high- and low-frequency cut-offs of the relaxation spectrum we consider here. Properties of such distribution functions are discussed by Gross (1947). In the present case

$$\mathscr{R}(t) = M_u \left[1 - C\int_{\tau_m}^{\tau_M} [1 - \exp(-t/\tau_\sigma)]\, D(\tau_\sigma)\, d\tau_\sigma\right] H(t), \tag{1.10}$$

so that

$$\mathscr{R}^*(s) = M_u \left[1 + C \ln \frac{s + \tau_M^{-1}}{s + \tau_m^{-1}}\right], \tag{1.11}$$

where $C = cD$. We observe that

$$\lim_{s\to\infty} \mathscr{R}^*(s) = M_u,$$

$$\lim_{s\to 0} \mathscr{R}^*(s) = M_u \left[1 - C \ln \frac{\tau_M}{\tau_m}\right] = M_R, \tag{1.12}$$

which defines M_R, the 'relaxed' modulus. Since we must have $M_R \geqslant 0$ we have the constraint

$$C \ln \frac{\tau_M}{\tau_m} < 1. \tag{1.13}$$

In other words, at fixed c, the relaxation spectrum ('absorption band', e.g. Anderson *et al.* 1977) cannot be too broad, nor can the density D be too high. In this paper, we are interested in the case where M_R is not too much smaller than M_u. (The constraint 1.13 stems specifically from our choice of M_u as a fundamental parameter. If M_R is fixed, then M_u may be unbounded.)

(b) Let us consider a one-dimensional wave propagation problem defined by the equation

$$\rho \frac{\partial^2 u}{\partial t^2} = \frac{\partial \sigma}{\partial x}, \tag{1.14}$$

where we assume that σ is related to $\epsilon = \partial u/\partial x$ by (1.1). We choose the following initial conditions and boundary conditions

$$\begin{cases} u(0, x) = 0; \quad \dfrac{\partial u}{\partial t}(0, x) = 0 \\ u(t, 0) = H(t); \quad \lim\limits_{x\to\infty} u(t, x) = 0. \end{cases} \tag{1.15}$$

The transformed problem reads

$$\begin{cases} \rho s^2 u^* - \mathscr{R}^* \dfrac{\partial^2 u^*}{\partial x^2} = 0, \\ u^*(s, 0) = 1. \end{cases} \tag{1.16}$$

We let $\mathscr{R}^*(s) = T^2(s)$ and choose the branch such that Re $T \geqslant 0$. The wave propagating in the positive x direction is given by

$$u^*(s, x) = \exp\left[-xs\sqrt{\rho}/T\right], \tag{1.17}$$

and the inversion integral is of the form

$$u(t, x) = \frac{1}{2i\pi}\int_{\gamma-i\infty}^{\gamma+i\infty} \frac{\exp(st)\,u^*(s, x)}{s}\,ds, \tag{1.18}$$

where the path of the integration runs to the right of the origin.

(c) The interpretation of the foregoing results for seismological applications is straightforward (e.g. Liu *et al.* 1976). Let $s = i\omega$ in (1.11), then

$$\mathscr{R}(\omega) = M_u\left[1 + C\ln\frac{i\omega + \tau_M^{-1}}{i\omega + \tau_m^{-1}}\right] \tag{1.19}$$

is the 'complex modulus'. The complex wave number is given by

$$k(\omega) = \omega\sqrt{\rho}/T(\omega) = \frac{\omega}{V_p(\omega)} - i\alpha(\omega), \tag{1.20}$$

where $V_p(\omega)$ is the frequency dependent phase velocity and $\alpha(\omega)$ the attenuation coefficient. The group velocity is given by

$$V_g^{-1}(\omega) = \mathrm{Re}\left[\frac{d}{d\omega}\left(\omega\sqrt{\rho}/T(\omega)\right)\right]. \tag{1.21}$$

Following Borcherdt (1973a), we define the quality factor by the formula

$$Q(\omega) = -\,\mathrm{Re}\,(k^2)/\mathrm{Im}\,(k^2), \tag{1.22}$$

which remains valid even for large attenuation. If in addition we assume that $C\ln(\tau_M/\tau_m) \ll 1$, then we have (Kolsky 1956)

$$Q^{-1} \simeq \tan\delta \sim C\tan^{-1}\frac{\omega(\tau_M - \tau_m)}{1 + \omega^2\tau_M\tau_m}, \tag{1.23}$$

where δ is the phase difference between a monochromatic stress wave and the associated strain. In that case Q^{-1} is essentially constant and equal to $C\pi/2$ in most of the range $\tau_M^{-1} \ll \omega \ll \tau_m^{-1}$, which is the main reason why the distribution (1.9) is attractive for seismological purposes (e.g. Liu *et al.* 1976).

2 The inversion internal

We have to evaluate the contour integral

$$u(t, x) = \frac{1}{2i\pi}\int_{\gamma-i\infty}^{\gamma+i\infty} \frac{\exp(st - sx\sqrt{\rho}/T)}{s}\,ds, \tag{2.1}$$

where

$$T^2(s) = M_u\left[1 + C\ln\frac{s + \tau_M^{-1}}{s + \tau_m^{-1}}\right]. \tag{2.2}$$

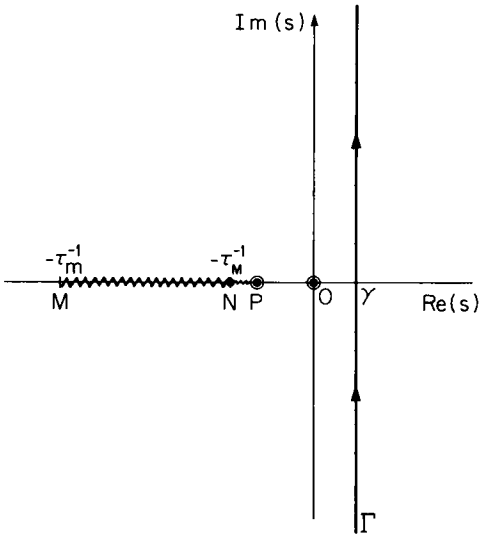

Figure 1. Geometry of the complex s plane.

The integrand is clearly analytic in the right half plane, which we know insures that the Kramers–Krönig relations and thus causality are satisfied (Kogan 1966a). We now investigate its behaviour for Re $s \leqslant 0$.

(a) The argument of the logarithm in (2.2) must not be real negative; we therefore introduce a branch cut along the segment $[-\tau_m^{-1}, -\tau_M^{-1}] = [\mathrm{M}, \mathrm{N}]$ of the real axis (Fig. 1). The principal branch of the logarithm is chosen. In addition, we assumed Re $T \geqslant 0$, which introduces a cut along [N, P] on the real axis, where the affix of P is

$$s(\mathrm{P}) = \frac{\tau_m^{-1} \exp(-1/C) - \tau_M^{-1}}{1 - \exp(-1/C)}. \tag{2.3}$$

Since C is small, P is to the right of N, but very close to it. P would approach the origin from the left if C ln τ_M/τ_m would become close to unity. The medium would then be fluid-like.

(b) The origin is a simple pole of the integrand with residue unity. Furthermore, T^2 vanishes at P so that P is an essential singularity. Since P is also a branch point, the exponent and the integrand do not afford Laurent series near P.

(c) As $|s| \to \infty$, $T \to \sqrt{M_u}$ so that the exponent in (2.1) takes the asymptotic form

$$F(s) = st - sx\sqrt{\rho}/T \sim s(t - x\sqrt{\rho/M_u}). \tag{2.4}$$

We introduce the notation $V_u = \sqrt{M_u/\rho}$, ('unrelaxed' wave velocity), and $t_u = x/V_u$, $\tau = t - t_u$.

For $\tau < 0$ the contour Γ may be deformed to infinity into the right half plane, and the integral vanishes. There is no signal prior to t_u.

For $\tau > 0$, the path Γ may be deformed into the left half plane. Contributions from arcs at infinity vanish exponentially, but non-zero contributions are expected from the various cuts and singularities in that case.

Because of the severe difficulties encountered in the close neighbourhood of P, we turn to asymptotic expansions to approximate (2.1). As shown by Brillouin (1960); Chu (1962) and Blake (1974), the most efficient approach in this case is the method of steepest descent. It requires finding the saddle points of the exponent $F(s)$.

A very detailed discussion of the methods used to approximate integrals such as (2.1) is provided by Elices & García-Moliner (1968). The general theory as well as special cases are treated by Baerwald (1930a, b, 1931).

We have

$$F(s) = t_u s\left[\frac{\tau}{t_u} + 1 - \left(1 + C\ln\frac{s+\tau_M^{-1}}{s+\tau_m^{-1}}\right)^{-1/2}\right] = t_u g(s), \tag{2.5}$$

and we seek an expansion valid for large values of t_u. The quantity τ/t_u is treated as a parameter in $g(s)$, and the saddle points are solutions of

$$\begin{aligned} g'(s) = \frac{dg}{ds} = \frac{\tau}{t_u} + 1 - \left(1 + C\ln\frac{s+\tau_M^{-1}}{s+\tau_m^{-1}}\right)^{-1/2} \\ + \frac{sC}{2}\left(1 + C\ln\frac{s+\tau_M^{-1}}{s+\tau_m^{-1}}\right)^{-3/2}\left(\frac{1}{s+\tau_M^{-1}} - \frac{1}{s+\tau_m^{-1}}\right) = 0. \end{aligned} \tag{2.6}$$

It is clear that for any real $s \in]P, +\infty[$, it is possible to find a real value of τ/t_u such that this equation be satisfied. There are therefore saddle points on the real axis, parameterized by τ/t_u. In order to find the direction of steepest descent, we need the second derivative

$$\begin{aligned} g''(s) = \frac{d^2g}{ds^2} = C\left(1 + C\ln\frac{s+\tau_M^{-1}}{s+\tau_m^{-1}}\right)^{-3/2}\left(\frac{1}{s+\tau_M^{-1}} - \frac{1}{s+\tau_m^{-1}}\right) \\ - \frac{Cs}{2}\left(1 + C\ln\frac{s+\tau_M^{-1}}{s+\tau_m^{-1}}\right)^{-3/2}\left(\frac{1}{(s+\tau_M^{-1})^2} - \frac{1}{(s+\tau_m^{-1})^2}\right) \\ - \frac{3C^2s}{4}\left(1 + C\ln\frac{s+\tau_M^{-1}}{s+\tau_m^{-1}}\right)^{-5/2}\left(\frac{1}{s+\tau_M^{-1}} - \frac{1}{s+\tau_m^{-1}}\right)^2. \end{aligned} \tag{2.7}$$

The first order of business is to search for possible saddle points elsewhere in the complex s plane. This is done in Appendix A, and we summarize the results as follows:

The only saddle point of interest s_0 lies on the real axis, to the right of P, and $g''(s_0)$ is positive so that the path of steepest descent is normal to the real axis at s_0.

For small values of τ, s_0 is large and positive; its value decreases as τ increases, vanishes for the critical value $\tau_R = t_R - t_u$, where $t_R = x\sqrt{\rho}/M_R$ is the 'relaxed' propagation time; s_0 approaches P from the right as τ becomes much larger than τ_R. A more detailed discussion is provided in Appendix A. Heuristically, the behaviour of s_0 as a function of τ means that the high frequency components of the signal, which travel at higher phase and group velocities arrive early. The 'infinite' frequency component arrives in fact at $\tau = 0$. On the other hand, low frequency components, with periods long compared to the longest relaxation time τ_M, will arrive at time τ_R, and will dominate the signal at large distances since they undergo little attenuation.

3 The transient response

3.1 THE PRECURSORS

According to the results of Appendix A, $g''(s_0)$ becomes very small as $\tau \to 0$ and s_0 becomes correspondingly large. The saddle point is very flat and we turn to a special approximation in that case. We shall use a device proposed by Sommerfeld (1914) and described by

Brillouin (1960), and distort the contour in the s-plane into a large circle $\mathscr{C}$, of radius r, surrounding the origin counterclockwise.

Contributions from arcs at infinity in the left half plane vanish, and contributions from the negative real axis, to the left of $\mathscr{C}$ (and of M) cancel each other out. Then, for large r,

$$g(s) \simeq \frac{\tau}{t_u} + \frac{C}{2}(\tau_M^{-1} - \tau_m^{-1}) - \frac{C}{4s}(\tau_M^{-2} - \tau_m^{-2}), \tag{3.1}$$

so that

$$u(t, x) \simeq \frac{\exp(Ct_u/2)(\tau_M^{-1} - \tau_m^{-1})}{2i\pi} \int_{\mathscr{C}} \frac{\exp[st + (Ct_u/4s)(\tau_m^{-2} - \tau_M^{-2})]\, ds}{s}. \tag{3.2}$$

We now operate the substitution $s = r\exp(i\phi)$ and choose $r = \sqrt{(Ct_u/4\tau)(\tau_m^{-2} - \tau_M^{-2})}$, valid for small τ/t_u, and thus

$$u(t, x) \simeq \exp\left[-\frac{C}{2}t_u(\tau_m^{-1} - \tau_M^{-1})\right] \frac{1}{\pi}\int_0^{\pi} \exp\left[\sqrt{C\tau t_u(\tau_m^{-2} - \tau_M^{-2})}\cos\phi\right] d\phi. \tag{3.3}$$

This integral is simply a representation of the modified Bessel function of order zero I_0 (e.g. Abramowitz & Stegun 1964; Jahnke & Emde 1945), so that

$$u(t, x) \simeq \exp\left[-\frac{C}{2}t_u(\tau_m^{-1} - \tau_M^{-1})\right] I_0\left[\sqrt{C\tau t_u(\tau_m^{-2} - \tau_M^{-2})}\right]$$

$$\simeq \exp\left[-\frac{C}{2}t_u(\tau_m^{-1} - \tau_M^{-1})\right]\left\{1 + \frac{C\tau t_u}{4}(\tau_m^{-2} - \tau_M^{-2}) + \left[\frac{C\tau t_u(\tau_m^{-2} - \tau_M^{-2})}{8}\right]^2 + O(\tau^3)\right\}. \tag{3.4}$$

We see that the signal does not vanish for $\tau = 0$, a result which could be obtained by use of a Tauberian theorem (e.g. Chu 1962). (3.4) shows that there remains a small step, the amplitude of which decreases exponentially as t_u becomes large.

For $C = 5 \times 10^{-3}$, $t_u = 10^3$ s, $\tau_m = 0.1$ s and τ_M large, $u(t_u^+, x) \simeq 10^{-11}$. This result is not altogether unexpected since we know the behaviour of the attenuation coefficient $\alpha(\omega)$ as $\omega \to \infty$ (e.g. Liu *et al.* 1976). We have

$$\alpha(\omega) = \omega\sqrt{\rho}\ \mathrm{Im}\left[\mathscr{R}^{-1/2}(\omega)\right], \tag{3.5}$$

where $\mathscr{R}(\omega)$ is given by (1.19). It is easy to verify that

$$\lim_{\omega\to\infty} \alpha(\omega) = \frac{C}{2V_u}(\tau_m^{-1} - \tau_M^{-1}). \tag{3.6}$$

Comparison with (3.4) shows that, as $\tau \to 0$, we find the original step function, considerably attenuated by the travel of duration $t_u = x/V_u$, through a medium with constant attenuation coefficient (3.6). This is where the 'infinite frequency component' of the signal is to be found, and it travels with the velocity V_u as expected.

The approximation is valid for $(\tau_m s)^{-1} \ll 1$, which requires $\tau/t_u \ll C/4$; with the values used previously, this means the first 1/10 of a second after t_u.

3.2 THE SIGNAL

We now turn to the integration of (2.1) in the vicinity of the saddle points described in Appendix A. The first difficulty raised by the present problem comes from the fact that, as

the saddle point migrates with varying τ, it may come indefinitely close to, and in fact merges with the pole at the origin. In that case, the straightforward saddle point approximation becomes inaccurate (e.g. Jeffreys & Jeffreys 1956). In order to obtain a uniform approximation, valid even for $\tau \sim \tau_R$, we resort to a device described by Ott (1943). Let s_0 be the saddle point and let

$$\xi^2 = -(s - s_0)^2 g''(s_0)$$

along the path of steepest descent approximated by its tangent at s_0. Then (2.1) may be approximated by

$$\begin{aligned} u(t, x) &\simeq \frac{\exp [t_u g(s_0)]}{2\pi} \int_{-\infty}^{+\infty} \frac{\exp(-t_u \xi^2/2}{s_0\sqrt{g''(s_0)} + i\xi} d\xi \\ &= \frac{\exp [t_u g(s_0)]}{2\pi} \int_{-\infty}^{+\infty} (s_0\sqrt{g''(s_0)} - i\xi) \frac{\exp(-t_u \xi^2/2)\, d\xi}{s^2 g''(s_0) + \xi^2}. \end{aligned} \tag{3.7}$$

The second term on the right-hand side vanishes on account of the parity of the integrand. The first term is readily evaluated from the formula (e.g. Abramowitz & Stegun 1964)

$$\int_0^\infty \frac{\exp(-at^2)}{t^2 + x^2} dt = \frac{\pi}{2x} \exp(ax^2) \operatorname{erfc}(x\sqrt{a}), \qquad (a, x > 0), \tag{3.8}$$

where erfc is the complementary error function, which takes the value 1 as its argument vanishes, while it vanishes exponentially for large argument. Taking into account the sign of s_0, as well as the contribution from the residue at the pole 0, we get

$$u(t, x) = H(-s_0) + \tfrac{1}{2} \operatorname{sgn}(s_0) \exp [\![t_u [g(s_0) + s_0^2 g''(s_0)/2]]\!] \operatorname{erfc} \sqrt{t_u s_0^2 g''(s_0)/2}, \tag{3.9}$$

where s_0 is an implicit function of τ.

This result is in agreement with the expression obtained by Chu (1962). The initial step function is degraded into a diffuse wave front. The half amplitude is reached at point x for $\tau = \tau_R(x)$, which corresponds to a propagation velocity of V_R. This is the result used by Blake (1974) and Blake & Dienes (1976).

Unfortunately we observe a discrepancy between the behaviour predicted by (3.9) and the numerical evaluation performed by Liu *et al.* (1976). Since the impulse response is obtained by differentiation of the transient response, one half of the area under the impulse response curve should be found for $t_u < t < t_R$, the other half for $t_R < t$. A rapid examination of the curve calculated by Liu *et al.* (1976), shown on Fig. 3, shows that more than half of the area appears to lie in the interval $t_u < t < t_R$. In fact, numerical evaluation of (3.9) and subsequent differentiation with respect to time (impulse response) yields anomalously high amplitudes for $t_R < t$.

The reason for this discrepancy may be understood on the basis of the results of Appendix A. The power series expansion of $g(s)$ near s_0 has only a radius of convergence $s_0 - s_p$. For s_0 small, the exponent $-t_u \xi^2/2$ may only take values of the order of $-Ct_u \tau_M^{-1}$ within the circle of convergence. This means that we can only expect (3.9) to be accurate for very large propagation times t_u. This is usually not the case for body wave seismology, where τ_M may well be greater than t_u.

In addition, the successive derivatives of g at s_0 become large as s_0 becomes small or negative; the path of steepest descent possesses sharp curvature at s_0 and bends over quickly into the negative real axis direction as sketched on Fig. 2.

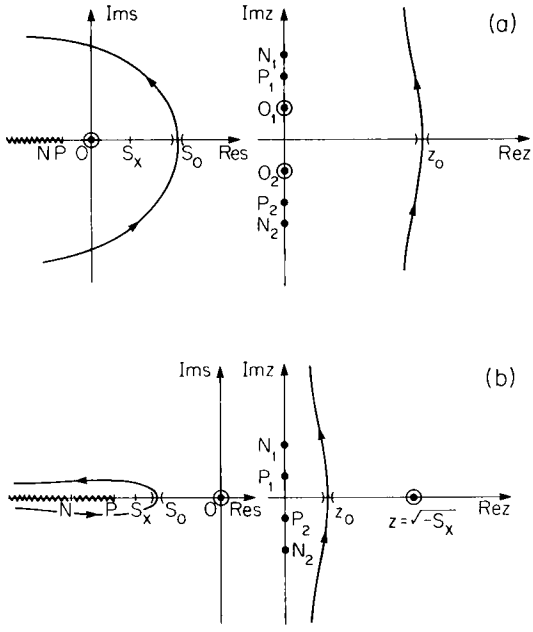

Figure 2. Mapping of the complex s plane into the half plane Re $z \geqslant 0$. Sketches are for the cases (a) $s_0 \gg 1$, (b) $s_0 < 0$. In both cases the path of steepest descent is sketched in each plane.

On the other hand, if $t_u \gg \tau_m$, for small τ, s_0 is large and positive and this difficulty does not arise, so that (3.9) is in fact a good 'first motion approximation' in that case.

Nevertheless, this approximation exhibits a satisfactory behaviour, at least qualitatively, as shown by Blake & Dienes (1976). This means that the parabolic approximation to $g(s)$ is reasonably good even outside the radius of convergence. This suggests that a better approximation may be obtained by correcting (3.9) for the curvature of the path near s_0. This is done by introducing the mapping

$$z^2 = s - s_x, \tag{3.10}$$

where s_x is the focus of the branch of hyperbola osculating the path at s_0. Let

$$f(z) = g[s(z)]. \tag{3.11}$$

The complex s plane, cut along the real axis to the left of s_x is mapped into the half plane Re $(z) > 0$ (Fig. 2). The cuts {MNP} are mapped along the imaginary axis, and we have

$$\left.\begin{aligned} f'(z) &= 2zg'(z^2 + s_x) \\ f''(z) &= 2g' + 4z^2 g'' \\ f'''(z) &= 12zg'' + 8z^3 g''' \end{aligned}\right\} \tag{3.12}$$

$$u(t, x) = \frac{1}{2i\pi} \int_{-\infty}^{+\infty} \frac{\exp\,[t_u f(z)]\; 2z dz}{z^2 + s_x}. \tag{3.13}$$

There is a saddle point at z_0 defined by $z_0^2 = s_0 - s_x$, the path of deepest descent cuts the real z axis at z_0 at right angles and can be extended to infinity in either imaginary direction.

The condition for the curvature of the path to vanish at z_0 is

$$\left.\begin{aligned} s_x &= s_0 + 3g''(s_0)/2g'''(s_0), \\ z_0^2 &= -3g''(s_0)/2g'''(s_0), \end{aligned}\right\} \tag{3.14}$$

where the necessary expressions are given in Appendix B. Then

$$f(z_0) = g(s_0); \quad f'(z_0) = 0; \quad f''(z_0) = 4z_0^2 g''(s_0); \quad f'''(z_0) = 0. \tag{3.15}$$

The substitution $\xi^2 = (z - z_0)^2 f''(z_0)$ in (3.13) leads to the saddle point approximation:

$$u(t, x) \simeq \frac{\exp\,[t_u f(z_0)]}{\pi} \int_{-\infty}^{+\infty} \frac{\exp\,(-t_u \xi^2/2)\,[z_0\sqrt{f''} + i\xi]}{[z_0\sqrt{f''} + i\xi]^2 + s_x f''}\, d\xi. \tag{3.16}$$

At this point we have to consider two cases, according to the sign of s_x.

(a) $s_x > 0$: $s_x = a^2$

This is the case for small values of τ. From Appendix A, we see that under the condition $\tau_m \ll \tau_M, t_u$, this case corresponds approximately to the condition

$$s_0 > \tau_m^{-1}/6, \quad \tau < 0.358\, t_u/Q_m. \tag{3.17}$$

By suitable changes of variables, and some manipulations of the integrand, (3.16) may be written in that case

$$\begin{aligned} u(t, x) = \frac{2}{\pi} \exp\,[t_u g(s_0)] \Bigg[Y \int_0^\infty \frac{[\eta^2 - (X^2 - Y^2)]\,\exp\,(-\eta^2)}{\eta^4 - 2(X^2 - Y^2)\eta^2 + (X^2 + Y^2)^2} d\eta \\ + X \int_0^\infty \frac{2XY \exp\,(-\eta^2)}{\eta^4 - 2(X^2 - Y^2)\,\eta^2 + (X^2 + Y^2)} \Bigg], \end{aligned} \tag{3.18}$$

where the odd powers of η in the numerator have been ignored because of parity, and where

$$\left.\begin{aligned} X &= az_0\sqrt{2t_u g''} \\ Y &= z_0^2\sqrt{2t_u g''} \end{aligned}\right\}. \tag{3.19}$$

The integrals appearing in (3.18) are known (e.g. Abramowitz & Stegun 1964) and we have

$$u(t, x) = \left[Y\,\mathrm{Re}\,\frac{w(X + iY)}{Y - iX} + X\,\mathrm{Im}\,\frac{w(X + iY)}{Y - iX} \right] \exp\,[t_u g(s_0)] = \exp\,(t_u g)\,\mathrm{Re}\,w(X + iY), \tag{3.20}$$

in which $w(z)$ is related to the complementary error function by

$$w(z) = \exp\,(-z^2)\,\mathrm{erfc}\,(-iz). \tag{3.21}$$

From (3.17) we see that (3.20) holds for very small times in most cases of interest.

(b) $s_x < 0$: $s_x = -a^2$

This is the case for larger values of τ. In that case we find

$$u(t, x) \simeq \frac{\exp\,[t_u g(s_0)]}{2\pi}\left[\int_{-\infty}^{+\infty} \frac{\exp\,(-t_u\xi^2/2)\,d\xi}{2(z_0+a)z_0\sqrt{g''+i\xi}} + \int_{-\infty}^{+\infty} \frac{\exp\,(-t_u\xi^2/2)\,d\xi}{2(z_0-a)z_0\sqrt{g''+i\xi}}\right]. \tag{3.22}$$

The integrals appearing here are of the same form as (3.7). Only the pole at $z = a$ will eventually yield a residue contribution, and the result takes the form:

$$\begin{aligned} u(t, x) = {} & H(a - z_0) + \tfrac{1}{2}\exp\,[\![t_u[g + 2z_0^2(z_0+a)^2 g'']]\!]\,\operatorname{erfc}\sqrt{2t_u z_0^2(z_0+a)^2 g''} \\ & + \tfrac{1}{2}\operatorname{sgn}(z_0 - a)\exp\,[\![t_u[g + 2z_0^2(z_0-a)^2 g'']]\!]\,\operatorname{erfc}\sqrt{2t_u z_0^2(z_0-a)^2 g''}. \end{aligned} \tag{3.23}$$

We see that in this approximation, $u(t_R, x) > \tfrac{1}{2}$; the wave is slightly sharper than predicted by (3.9).

One interesting limiting case is $C \ln(\tau_M/\tau_m) \to 1$; in that case the material is fluid-like and $P \to 0, a \to 0$, then

$$u(t, x) \sim \exp\,[t_u(g + 2z_0^4 g'')]\,\operatorname{erfc}\sqrt{2t_u z_0^4 g''}. \tag{3.24}$$

This is precisely the expression derived by Chu (1962) for fluid-like materials. The wave propagates as a diffusion wave in an elastoviscous fluid-like medium.

One may also show that (3.20) and (3.23) tend to (3.9) in the limit of very large t_u.

Although the expressions just derived represent better approximations, the problem raised earlier about the circle of convergence for the Taylor expansion of the exponent has not been removed. Significant contributions from portions of the path lying outside the circle of convergence will arise for large values of τ. The quality of the approximation is most easily evaluated numerically in that case (e.g. Strick 1970), by recomputing the Laplace transform and direct comparison with the theoretical function $u^*(s, x)$. Better approximations will most likely require a different approach from the one used here, which may be qualified as a 'first motion' approximation.

4 The impulse response

For seismological purposes, instead of the transient response $u(t, x)$, it is more convenient in many cases to consider an impulse response, whereby the boundary condition at $x = 0$ involves a delta function rather than a step function.

We derive an asymptotic expression for this impulse response $v(t, x)$ by differentiating $u(t, x)$ with respect to time (e.g. Courant & Hilbert 1953).

4.1 THE PRECURSOR

For very small values of τ/t_u, we obtain from (3.4)

$$\begin{aligned} v(t, x) = {} & \exp\,[-(C/2)t_u(\tau_m^{-1} - \tau_M^{-1})]\,\delta(\tau) \\ & + \frac{Ct_u}{4}(\tau_m^{-2} - \tau_M^{-2})\exp\,[-(C/2)t_u(\tau_m^{-1} - \tau_M^{-1})]\left[1 + \frac{Ct_u}{8}(\tau_m^{-2} - \tau_M^{-2})\tau + 0(\tau^2)\right]. \end{aligned} \tag{4.1}$$

There appears to be a very small Dirac impulse at time $t = t_u$, which corresponds to the propagation of the very high frequencies at velocity V_u, but attenuated by a constant

attenuation, as shown in (3.6). Then follows a small amplitude precursor, just as in the case of the transient response $u(t, x)$, and finally the 'visible part' of the wave.

The existence of a Dirac impulse at $t = t_u$ may also be derived from the following asymptotic behaviour

$$v^*(s, x) \simeq \exp(-st_u) \exp[-(C/2)\, t_u(\tau_m^{-1} - \tau_M^{-1})], \quad s \gg 1, \tag{4.2}$$

which may be obtained directly from (1.17). This term will be important whenever $C \ll 1$, that is, for very low loss media, and when τ_m is not very small. It must be introduced in numerical checks involving a recomputation of the Laplace transform of the asymptotic signal. For long travel time, or high attenuation, this term is obviously negligible.

4.2 THE SIGNAL

The main portion of the pulse is obtained by time differentiation of (3.20) and (3.23). We shall need the following results

$$\frac{ds_0}{dt} = \dot{s}_0 = -\frac{1}{t_u g''}. \tag{4.3}$$

$$\frac{d(t_u g)}{dt} = s_0, \tag{4.4}$$

$$\dot{z}_0 = \frac{3}{4t_u z_0 g''}\left(1 + \frac{2}{3} z_0^2 \frac{g^{(4)}}{g'''}\right), \tag{4.5}$$

$$\dot{s}_x = \dot{s}_0 - 2z_0 \dot{z}_0, \tag{4.6}$$

$$\frac{dw(\zeta)}{d\zeta} = -2\zeta w(\zeta) + \frac{2i}{\sqrt{\pi}}, \tag{4.7}$$

$$\frac{d}{d\zeta}\operatorname{erfc}(\zeta) = -\frac{2}{\sqrt{\pi}} \exp(-\zeta^2). \tag{4.8}$$

Again, we distinguish two cases:

(a) $s_x = a^2$

Then by differentiation of X^2 and Y^2, we obtain

$$\dot{X} = \frac{\dot{a}}{a} X, \qquad \dot{Y} = \frac{\dot{z}_0}{z_0} Y, \tag{4.9}$$

so that

$$v(t, x) = (z_0^2 + a^2)\, u(t, x) + \exp(t_u g) \operatorname{Re}\left\{\left[-2(X + iY) w(X + iY) + \frac{2i}{\sqrt{\pi}}\right](\dot{X} + i\dot{Y})\right\}. \tag{4.10}$$

(b) $s = -a^2$

Then we find

$$\frac{d}{dt}[2t_u(z_0 \pm a)^2 z_0^2 g''] = \pm z_0 \frac{z_0 \pm a}{a}\left[5z_0 \pm 3a + 2z_0^2(z_0 \pm a)\frac{g^{(4)}}{g'''}\right], \tag{4.11}$$

and, by differentiation of (3.23)

$$v(t,x) = \frac{(z_0+a)^2}{2a}\left[5z_0 - a + 2z_0^3\frac{g^{(4)}}{g'''}\right]\exp\left[\left[t_u\left[g + 2z_0^2(z_0+a)^2g''\right]\right]\right.$$
$$\times \operatorname{erfc}\sqrt{2t_u z_0^2(z_0+a)^2 g''} + \operatorname{sgn}(z_0-a)\frac{(z_0-a)^2}{2a}\left[5z_0+a+2z_0^3\frac{g^{(4)}}{g'''}\right] \qquad (4.12)$$
$$\left.\times \exp\left[\left[t_u\left[g + 2z_0^2(z_0-a)^2g''\right]\right]\right] \operatorname{erfc}\sqrt{2t_u z_0^2(z_0-a)^2 g''} - \frac{3+2z_0^2 g^{(4)}/g'''}{\sqrt{2\pi t_u g''}}\exp(t_u g).\right.$$

For τ_m not too small, (4.10) represents the major part of the pulse; this is also true if Q_m is large (low attenuation). In other cases, (4.12) is the appropriate expression to represent the signal.

These expressions were checked against the results of numerical differentiation of $u(t, x)$. It was found that numerical differentiation is actually quite adequate in many cases, but that the results given above are required in the case of high Q_m, or relatively large τ_m.

5 A numerical example

In order to illustrate the results derived in the previous section, we give here a brief comparison of waveforms calculated using our approximation with previously published waveforms. The transient response was calculated according to the results of Section 3, and the impulse response according to the results of Section 4. The parameters were chosen to match the calculation of Liu *et al.* (1976), and the results are plotted on Fig. 3. Numerical values of the parameters were chosen as follows:

$\tau_m = 0.0037$ s, $\tau_M = 7250$ s, $Q_m = 98.413$, $t_u = 373.4$ s.

The corresponding frequency dependence of Q, as well as the dispersion curves were published by Liu *et al.* (1976) and will not be duplicated here.

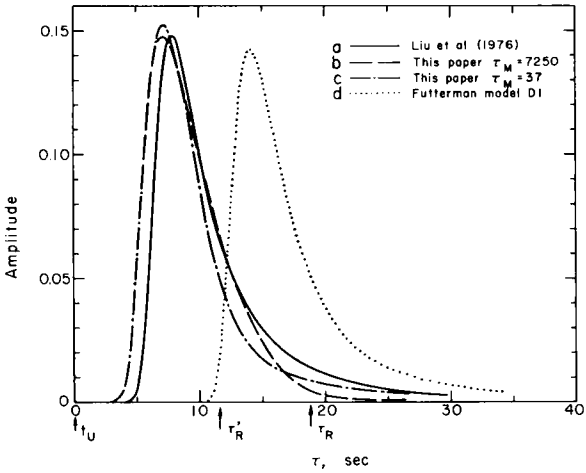

Figure 3. Impulse responses for $t_u = 373.4$ s, $Q_m = 98.413$, $t_m = 0.0037$ s. (a) $\tau_M = 7250$ s, calculation of Liu *et al.* (1976). (b) $\tau_M = 7250$ s, this paper. (c) $\tau_M = 37$ s, this paper. (d) Futterman (1962), Model D1 (arbitrarily shifted for clarity). τ_R and τ'_R are the 'relaxed' arrival times for $\tau_M = 7250$ s, and $\tau_M = 37$ s respectively.

The curves depicted on Fig. 3 correspond to the following calculations:

Curve (a). This is the result obtained by Liu *et al.* (1976) using an FFT method.
Curve (b). Is the impulse response derived on the basis of the present work.
Curve (c). Is also derived from the present work, but with $\tau_M \sim t_u/10 \sim 37$ s.

These three curves are plotted as functions of $\tau = t - t_u$, with a common amplitude scale (i.e. they were not normalized). The 'relaxed' times $\tau_R \simeq 19.8$ s for curves (a) and (b) and $\tau'_R \sim 11.6$ s for curve (c) are also indicated on the figure. The last curve (d) corresponds to Futterman's (1962) model D1 and is given here for comparison. Since Futterman chose V_R as his reference velocity, and assumes that the absorption band extends to very high frequencies, V_u is not bounded for his model, and t_u is ill defined; therefore curve (d) was arbitrarily shifted along the time axis for clarity.

Some of the characteristic parameters for the various pulses are listed below:

	a	*b*	*c*
Visual onset (s)	4.15	3.27	3.27
Peak time (s)	7.9	7.2	7.2
Rise time (s)	2.0	2.0	2.0
Peak amplitude	0.148	0.148	0.152
Half amplitude width (s)	5.0	6.0	5.1

Comparison of the three curves is very favourable. The only significant differences appear in the decay of the pulse. This confirms our conclusion that our analysis yields a good first motion approximation but that the quality of the approximation deteriorates for long times.

It is significant to note that the onset time for curve (a) corresponds to a signal velocity equal to the phase velocity at 4.096 Hz, which is the highest frequency taken into account by Liu *et al.* in their FFT calculation (Liu, private communication). This points out the advantage of analytical approaches such as ours when high frequencies are to be considered. The 'frontal' part of the pulse is essentially controlled by the value of τ_m, and is practically insensitive to τ_M. The same holds for the amplitude. In particular, the duration of the very low amplitude precursor is very sensitive to τ_m and C, so that one may expect that comparison of observed travel times for short period body waves with results from long period seismology will eventually permit us to place a bound on τ_m.

It is of interest to note that waveform (c) is closer in shape to (a) than (b) is. This implies that relaxation mechanisms with a relaxation time of the order of or greater than t_u have actually a rather negligible effect on the attenuated pulse shape. This result is intuitively satisfying in as much as slow relaxation mechanisms do not have time to operate for short travel times. On the other hand, it can be said that the long time decay of curve (b) is too rapid so that the pulse width is too large and the amplitude at τ_R too small. This clearly expresses the loss of accuracy of our approximation for long times when $t_u < \tau_M$. Laplace transforms of curves (b) and (c) were calculated numerically using a simple trapezoidal integration scheme, and compared to the theoretical transform. The error for curve (b) was at most 4 per cent, and for curve (c) was nowhere greater than 0.7 per cent. However, the difference between the two analytical transforms was only two per cent for intermediate values of the Laplace variable s, so the curve (c) is actually a better overall approximation to the solution at intermediate to large times than curve (b) is. This is additional evidence that the long period extremity of the absorption band cannot be easily investigated by studying pulse shapes; as one would expect on physical grounds, information about τ_M will rather come from the study of long period phenomena, such as free oscillations (e.g. Kanamori & Anderson 1977; Anderson & Hart 1977).

Stacey *et al.* (1975) proposed a set of criteria that attenuated pulse models should satisfy in order to be acceptable for geophysical purposes. Futterman's model D1 – curve (d) on Fig. 3 – was found to satisfy these criteria except for the fact that the visual onset time was earlier than what one would calculate from the 'elastic' velocity. As pointed out by Savage (1976), and Liu *et al.* (1976) it cannot be claimed that this is a failure of Futterman's model because of this author's choice of V_R as the 'elastic' velocity. This source of possible confusion is removed from our present investigation and the standard linear solid model, as proposed by Liu *et al.* (1976) does not violate any of the criteria developed by Stacey *et al.*

Conclusion

The focus of this paper has been on the analysis of the plane wave propagation problem in a standard linear solid. The classical asymptotic approximation to the transient and impulse responses is valid for very long travel times. We have shown that by suitable modification of the method of steepest descent, the range of validity of the approximation may be extended to shorter travel times in the form of a first motion approximation.

This analytical approach allowed us to investigate the nature and behaviour of the low amplitude precursor to the attenuated pulse and to obtain a better estimate of the signal velocity, based on the 'visual' onset of the pulse. The second part of this research, to be published in a separate paper will consist of a parameter study of the characteristics of such attenuated pulses and a discussion of some of their seismological implications.

Acknowledgments

Numerous and fruitful discussions with H. Kanamori, D. Anderson, G. Mellman, and A. Suteau about various aspects of this work, as well as a detailed review by V. Cormier, are gratefully acknowledged.

This research was supported by the Advanced Research Projects Agency of the Department of Defense and was monitored by the Air Force Office of Scientific Research under Contract No. AFOSR F49620-77-C-0022. Contribution No. 2898, Division of Geological and Planetary Sciences, Seismological Laboratory, California Institute of Technology, Pasadena, California.

Since the completion of this work, I became familiar with the independent work of R. Chin & L. Thigpen (1977). These authors obtained results which are generally compatible with the present work and provide some interesting extensions, particularly with regard to the construction of uniformly asymptotic expansions. Very instructive discussions with these authors are gratefully acknowledged.

References

Abramowitz, M. & Stegun, I. A., 1964. *Handbook of mathematical functions,* National Bureau of Standards.

Anderson, D. L., 1967. The anelasticity of the mantle, *Geophys. J. R. astr. Soc.*, **14**, 135–164.

Anderson, D. L. & Hart, R. S., 1977. The *Q* of the Earth, *J. geophys. Res.*, in press.

Anderson, D. L., Kanamori, H., Hart, R. S. & Liu, H.-P., 1977. The Earth as a seismic absorption band, *Science*, **196**, 1104–1106.

Azimi, Sh. A., Kalinin, A. V. & Pivovarov, B. L., 1968. Impulse and transient characteristics of media with linear and quadratic absorption laws, *Izv. Earth Phys.*, **2**, 42–54 (English Translation).

Baerwald, H. G., 1930a. Über die Fortpflanzung von Signalen in dispergierenden Systemen – Erster Teil, *Ann. Phys.*, **6**, 295–369.

Baerwald, H. G., 1930b. Über die Fortpflanzung von Signalen in dispergierenden Systemen, Zweiter Teil, *Ann. Phys.*, **7**, 731–760.

Baerwald, H. G., 1931. Über die Fortpflanzung von Signalen in dispergierenden Systemen, Dritter Teil, *Ann. Phys.*, **8**, 565–614.

Blake, T. R., 1974. The response of a linear viscoelastic solid to a weak spherical explosion, *Bull. seism. Soc. Am.*, **64**, 1697–1705.

Blake, T. R. & Dienes, J. K., 1976. On viscosity and the inelastic nature of waves in geological media, *Bull. seism. Soc. Am.*, **66**, 453–465.

Borcherdt, R. D., 1973a. Energy and plane wave in linear viscoelastic media, *J. geophys. Res.*, **78**, 2442–2453.

Borcherdt, R. D., 1973b. Rayleigh-type surface wave on a linear viscoelastic half space, *J. acoust. Am.*, **54**, 1651–1653.

Borcherdt, R. D., 1977. Reflection and refraction of Type II *S* waves in elastic and anelastic media, *Bull. seism. Soc. Am.*, **67**, 43–68.

Brillouin, L., 1960. *Wave propagation and group velocity*, Academic Press, New York.

Buchen, P. W., 1971. Reflection, transmission and diffraction of *SH* waves in linear viscoelastic solids, *Geophys. J. R. astr. Soc.*, **25**, 97–113.

Carpenter, E. W., 1967. Teleseismic signals calculated for underground, underwater, and atmospheric explosions, *Geophysics*, **32**, 17–32.

Chin, R. C. Y. & Thigpen, L., 1977. Modeling waves in a linear viscoelastic medium, *Trans. Am. geophys. Un.*, **58**, 439.

Chu, B. T., 1962. Stress waves in isotropic linear viscoelastic materials, *J. de Mécanique*, **1**, 439–462.

Courant, R. & Hilbert, D., 1953. *Methods of mathematical physics*, Interscience, New York.

Elices, M. & García-Moliner, F., 1968. Wave packet propagation and frequency-dependent internal friction, in *Physical acoustics, V*, ed. Mason, Academic Press, New York.

Futterman, W. I., 1962. Dispersive body waves, *J. geophys. Res.*, **67**, 5279–5291.

Gross, B., 1947. On creep and relaxation, *J. appl. Phys.*, **18**, 212–221.

Gurevich, G. I., 1964. A basic feature of the propagation and attenuation of seismic vibrations, in *Aspects of the dynamic theory of seismic wave propagation collection vol. 7*, Sbornik.

Jackson, D. D. & Anderson, D. L., 1970. Physical mechanisms of seismic wave attenuation, *Rev. Geophys. Space Phys.*, **8**, 1–63.

Jahnke, E. & Emde, F., 1945. *Tables of functions*, Dover.

Jeffreys, H. & Jeffreys, B. S., 1956. *Methods of mathematical physics*, Cambridge University Press.

Kanamori, H. & Anderson, D. L., 1977. Importance of physical dispersion in surface wave and free oscillation problems: review, *Rev. Geophys. Space. Phys.*, **15**, 105–112.

Kogan, S. Ya., 1966a, b. A brief review of seismic wave absorption theories, I, and II, *Izv. Earth Phys.*, **11**, 3–28 (English Translation).

Kolsky, H., 1956. The propagation of stress pulses in viscoelastic solids, *Phil. Mag.*, **8**, 693–710.

Lamb, G. L., 1962. The attenuation of waves in a dispersive medium, *J. geophys. Res.*, **67**, 5273–5278.

Liu, H.-P., Anderson, D. L. & Kanamori, H., 1976. Velocity dispersion due to anelasticity: implications for seismology and mantle composition, *Geophys. J. R. astr. Soc.*, **47**, 41–58.

Lomnitz, C., 1957. Linear dissipation in solids, *J. appl. Phys.*, **28**, 201–205.

Malvern, L. E., 1969. *Introduction to the mechanics of a continuous medium*, Prentice Hall.

Ott, H., 1943. Die Sattelpunktsmethode in der Umgebung eines Pols Mit Anwendungen auf die Wellenoptik and Akustik, *Ann. Phys.*, **5**, 43, 393–403.

Rivlin, R. S., 1965. Nonlinear viscoelastic solids, *SIAM Rev.*, **7**, 323–340.

Savage, J. C., 1965. Attenuation of elastic waves in granular mediums, *J. geophys. Res.*, **70**, 3935–3942.

Savage, J. C., 1976. Anelastic degradation of acoustic pulses in rock – Comments, *Phys. Earth planet. Int.*, **11**, 284–285.

Schoenberg, M., 1971. Transmission and reflection of plane waves at an elastic–viscoelastic interface, *Geophys. J. R. astr. Soc.*, **25**, 35–47.

Sommerfeld, A., 1914. *Ann. d. Physik*, **44**, 177, presented in: Brillouin, L., 1960. *Wave propagation and group velocity*, Academic Press, New York.

Stacey, F. D., Gladwin, M. T., McKavanagh, B., Linde, A. T. & Haste, L. M., 1975. Anelastic damping of acoustic and seismic pulses, *Geophys. Surv.*, **2**, 133–151.

Strick, E., 1970. A predicted pedestal effect for pulse propagation in constant-Q solids, *Geophysics*, **35**, 387–403.

Appendix A

In this appendix we investigate the saddle points discussed in Section 2. The problem is to solve equation (2.6) in the complex s plane. We shall assume that $\tau_m \ll \tau_M$, which does not restrict the generality of the present investigation and provides the greatest range of possible cases.

A1 Saddle points near the origin

In that case we write

$$\left(1 + C \ln \frac{s + \tau_M^{-1}}{s + \tau_m^{-1}}\right)^{\alpha} = \left(\frac{M_R}{M_u}\right)^{\alpha} \left(1 + C \frac{M_u}{M_R} \ln \frac{1 + \tau_M s}{1 + \tau_m s}\right)^{\alpha} \simeq \left(\frac{M_u}{M_R}\right)^{\alpha} \left(1 + \alpha C \frac{M_u}{M_R} \ln \frac{1 + \tau_M s}{1 + \tau_m s}\right). \quad \text{(A1)}$$

The approximation requires

$$\left.\begin{aligned} -\frac{1}{C} &\ll \ln |s + \tau_M^{-1}| \\ -\frac{1}{C} &\ll \ln |s + \tau_m^{-1}| \end{aligned}\right\} \quad \text{(A2)}$$

which forbids very small domains surrounding M and N, (including P which is very close to N), because C is small. We may also assume that $|\tau_m s| \ll 1$ so that (2.6) becomes

$$\frac{\tau}{t_u} + 1 - \sqrt{\frac{M_u}{M_R}} + \frac{C}{2} \left(\frac{M_u}{M_R}\right)^{3/2} \left(\ln (1 + \tau_M s) + \frac{\tau_M s}{1 + \tau_M s}\right) = 0. \quad \text{(A3)}$$

Fig. A1 shows τ/t_u as a function of s, for s real, as calculated from (2.6) and (A3). The approximation is good for small values of s, that is, large values of τ/t_u. This is therefore a 'long time' approximation.

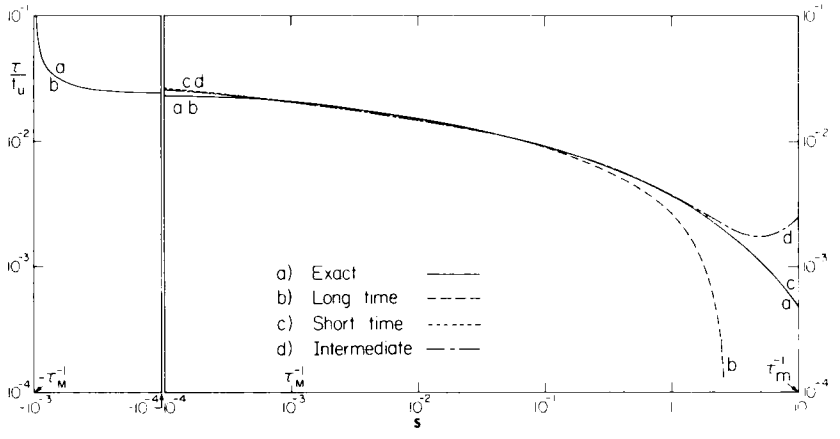

Figure A1. τ/t_u as a function of s, for $\tau_M = 0.1$ s, $\tau_M = 1000$ s, $C = 0.005$. (a) Exact solution (equation 2.6). (b) Long time approximation (equation A3). (c) Short time approximation (equation A7). (d) Intermediate times approximation (equation A10).

We rewrite (A3) in the form

$$\ln(1+\tau_M s) = \frac{1}{1+\tau_M s} - 1 - \frac{2}{C}\left(\frac{M_R}{M_u}\right)^{3/2}\left[\frac{\tau}{t_u} + 1 - \sqrt{\frac{M_u}{M_R}}\right], \tag{A4}$$

and set $1+\tau_M s = \rho \exp(i\phi)$. Equating the imaginary parts, we get

$$\phi = -\rho^{-1}\sin\phi,$$

which can only be satisfied for $\phi = 0$. The only saddle points in the vicinity of the origin are real. The two sides of (A4) are plotted on Fig. A2 as functions of $(1+\tau_M s)$. For any value of τ/t_u there is a unique saddle point s_0 such that $(V_R = \sqrt{M_R/\rho})$

$$s_0 > 0 \quad \text{for} \quad \frac{\tau}{t_u} < \frac{V_u - V_R}{V_R},$$

$$s_0 < 0 \quad \text{for} \quad \frac{\tau}{t_u} > \frac{V_u - V_R}{V_R}.$$

The constraint (A2) implies that

$$\frac{\tau}{t_u} \ll \frac{C}{2}\left(\frac{M_u}{M_R}\right)^{3/2} \exp(1/C),$$

which is always satisfied for seismological purposes. The critical value of τ/t_u, for which the saddle point is at 0 may be computed directly from (2.6) and is given by

$$\tau_R = t_R - t_u = \frac{x}{V_R} - \frac{x}{V_u}. \tag{A5}$$

From (2.7) we find

$$g''(s) \simeq \frac{C}{2}\left(\frac{M_u}{M_R}\right)^{3/2} \frac{\tau_M(2+\tau_M s)}{(1+\tau_M s)^2}. \tag{A6}$$

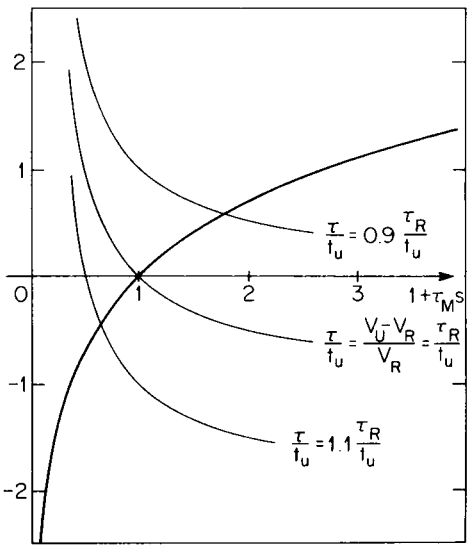

Figure A2. Graphical solution of equation (A4).

This function is positive along the real axis; the path of steepest descent runs parallel to the imaginary axis. From Fig. A1 it is clear that this approximation breaks down when s becomes much larger than τ_M^{-1}.

A2 Saddle points at intermediate distance from the origin

Because $\tau_m \ll \tau_M$ there is an annular region of the s plane for which $|\tau_m s| \ll 1 \ll |\tau_M s|$. In this case the proper approximation to (2.6) is

$$\frac{\tau}{t_u} + \frac{C}{2}(\ln \tau_m s - 2\tau_m s + 1) = 0. \tag{A7}$$

Letting $s = \rho \exp(i\phi)$ and equating imaginary parts for $\phi \neq 0$ we get

$$\tau_m \rho = \frac{\phi}{2 \sin \phi},$$

which corresponds to the minimum of the curve representing (A7) on Fig. 4. Then $\tau_m s = ½$ mation for $\phi \neq 0$. For s real, both sides of (A7) are plotted against $\tau_m s$ on Fig. A3. There is only one solution with $\tau_m s \ll 1$. In order to have a solution at all, we require

$$\frac{\tau}{t_u} > C\frac{\ln 2}{2},$$

which corresponds to the minimum of the curve representing (A7) on Fig. 4. Then $\tau_m s = ½$ and the approximation is not good unless $\tau/t_u > 0.35\,C$.

In the present case, we have

$$g''(s) = -\frac{C}{2}\left(2\tau_m - \frac{1}{s}\right), \tag{A8}$$

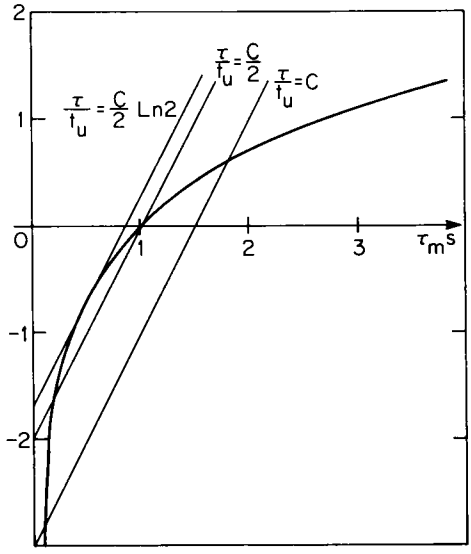

Figure A3. Graphical solution of equation (A7).

which is positive whenever the approximation is meaningful. The path is perpendicular to the real axis.

For smaller values of τ, we turn to yet another approximation.

A3 Saddle points away from the origin

In this case $|\tau_M s| \gg 1$ and

$$\left(1 + C \ln \frac{s + \tau_M^{-1}}{s + \tau_m^{-1}}\right)^{\alpha} \simeq 1 + \alpha C \ln \frac{s + \tau_M^{-1}}{s + \tau_m^{-1}} \tag{A9}$$

(2.6) is then approximated by

$$\frac{\tau}{t_u} - \frac{C}{2}\left[\ln \frac{1 + \tau_m s}{\tau_m s} + \frac{\tau_m s}{1 + \tau_m s} - 1\right] = 0. \tag{A10}$$

The corresponding curve on Fig. A1, valid for s real, shows that the approximation is clearly very good for large s, or small τ/t_u. This is a 'small time' approximation. Away from the real axis, we write (A10) as

$$\ln\left[1 + (\tau_m s)^{-1}\right] = \frac{-1}{1 + (\tau_m s)^{-1}} + 1 + \frac{2\tau}{C\tau_u} \tag{A11}$$

Let $1 + (\tau_m s)^{-1} = \rho \exp(i\phi)$, equate real and imaginary parts, so that

$$\left.\begin{aligned} \ln \rho &= -\rho^{-1} \cos\phi + 1 + \frac{2\tau}{Ct_u} \\ \phi &= \rho^{-1} \sin\phi \end{aligned}\right\}. \tag{A12}$$

This system has solutions for $\phi \neq 0$ only if $\tau < 0$. Again there are only real solutions. For s real, the two sides of (2.19) are plotted as functions of $1 + (\tau_m s)^{-1}$ on Fig. A4. For $\tau = 0$, there is a double solution $(\tau_m s)^{-1} = 0$; the saddle points are at infinity. For $\tau > 0$, we have two solutions, one for $s > 0$, to the right of P, and one for $s < 0$, to the left of M. As τ/t_u

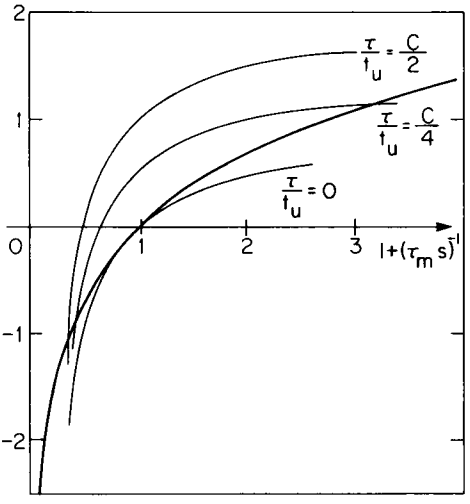

Figure A4. Graphical solution of equation (A11).

increases, the first saddle point approaches the origin from the right, the second one approaches M from the left, until the approximation becomes poor and we must revert to one of the former cases. From (2.7) we have

$$g''(s) \simeq \frac{C}{2s(1+\tau_m s)^2}. \tag{A13}$$

The saddle point for which $s_0 > 0$ is of the type encountered before. The path runs through the second saddle point along the real axis, however; but, because the solution must be real, and by reason of symmetry, Γ must be distorted symmetrically with respect to the real axis. It will then run twice through this second saddle point, once in each direction, and no contribution will arise.

In summary, the only saddle point of interest is real, to the right of P, and the path cuts the axis at right angles. For any given acceptable value s, τ/t_u calculated from (2.6) gives the time at which the saddle point is at s.

Appendix B

We give here the expressions to calculate the successive derivatives of $g(s)$.

Define

$$\left.\begin{aligned} \alpha &= \frac{1}{s+\tau_M^{-1}} & \alpha' &= -\alpha^2 \\ \beta &= \frac{1}{s+\tau_m^{-1}} & \beta' &= -\beta^2 \\ \gamma &= 1 + C\ln\frac{\beta}{\alpha} & \gamma' &= C(\alpha-\beta) \end{aligned}\right\}. \tag{B1}$$

Then we may derive the following expressions

$$g = s\left(\frac{\tau}{t_u} + 1 - \gamma^{-1/2}\right) \tag{B2}$$

$$g' = \frac{\tau}{t_u} + 1 - \gamma^{-1/2} + \frac{Cs}{2}\gamma^{-3/2}(\alpha-\beta) \tag{B3}$$

$$g'' = \frac{C}{2}\gamma^{-3/2}(\alpha-\beta)(2-\alpha s-\beta s) - \frac{3C^2}{4}\gamma^{-5/2}(\alpha-\beta)^2 s \tag{B4}$$

$$\begin{aligned} g''' = {} & \frac{C}{2}\gamma^{-3/2}(\alpha-\beta)(2\alpha^2 s + 2\alpha\beta s + 2\beta^2 s - 3\alpha - 3\beta) \\ & + \frac{9}{4}C^2\gamma^{-5/2}(\alpha-\beta)^2(\alpha s + \beta s - 1) + \frac{15}{8}C^3\gamma^{-7/2}(\alpha-\beta)^3 s \end{aligned} \tag{B5}$$

$$\begin{aligned} g^{(4)} = {} & C\gamma^{-3/2}(\alpha-\beta)(4\alpha^2 + 4\alpha\beta + 4\beta^2 - 3\alpha^3 s - 3\alpha^2\beta s - 3\alpha\beta^2 s - 3\beta^3 s) \\ & - \frac{3}{4}C^2\gamma^{-5/2}(\alpha-\beta)^2(11\alpha^2 s + 14\alpha\beta s + 11\beta^2 s - 12\alpha - 12\beta) \\ & - \frac{15}{4}C^3\gamma^{-7/2}(\alpha-\beta)^3(3\alpha s + 3\beta s - 1) - \frac{105}{16}C^4\gamma^{-9/2}(\alpha-\beta)^4 s. \end{aligned} \tag{B6}$$

In addition, we have

$$\left.\begin{aligned} f(z) &= g(z^2 + s) \\ f'(z) &= 2zg' \\ f''(z) &= 2g' + 4z^2 g'' \\ f'''(z) &= 12zg'' + 8z^3 g''' \\ f^{(4)}(z) &= 12g' + 48z^2 g''' + 16z^4 g^{(4)} \end{aligned}\right\}. \tag{B7}$$